

Clinical neuroanatomy

Dorsal and ventral language pathways in persistent developmental stuttering

Vered Kronfeld-Duenias^{a,*}, Ofer Amir^b, Ruth Ezrati-Vinacour^b,
Oren Civier^a and Michal Ben-Shachar^{a,c,*}

^a The Gonda Multidisciplinary Brain Research Center, Bar-Ilan University, Ramat-Gan, Israel

^b The Department of Communication Disorders, Sackler Faculty of Medicine, Tel-Aviv University, Israel

^c The Department of English Literature and Linguistics, Bar-Ilan University, Ramat-Gan, Israel

ARTICLE INFO

Article history:

Received 9 July 2015

Reviewed 6 September 2015

Revised 20 November 2015

Accepted 1 April 2016

Action editor Marco Catani

Published online 12 April 2016

Keywords:

White matter

Diffusion imaging

Stuttering

Tractography

Language pathways

ABSTRACT

Persistent developmental stuttering is a speech disorder that affects an individual's ability to fluently produce speech. While the disorder mainly manifests in situations that require language production, it is still unclear whether persistent developmental stuttering is indeed a language impairment, and if so, which language stream is implicated in people who stutter. In this study, we take a neuroanatomical approach to this question by examining the structural properties of the dorsal and ventral language pathways in adults who stutter (AWS) and fluent controls. We use diffusion magnetic resonance imaging and individualized tract identification to extract white matter volumes and diffusion properties of these tracts in samples of adults who do and do not stutter. We further quantify diffusion properties at multiple points along the tract and examine group differences within these diffusivity profiles. Our results show differences in the dorsal, but not in the ventral, language-related tracts. Specifically, AWS show reduced volume of the left dorsal stream, as well as lower anisotropy in the right dorsal stream. These data provide neuroanatomical support for the view that stuttering involves an impairment in the bidirectional mapping between auditory and articulatory cortices supported by the dorsal pathways, not in lexical access and semantic aspects of language processing which are thought to rely more heavily on the left ventral pathways.

© 2016 Elsevier Ltd. All rights reserved.

Persistent developmental stuttering is a speech disorder that affects verbal fluency in about 1% of the adult population. While the main manifestation of persistent developmental stuttering is the difficulty to fluently produce speech, it is still unclear whether this disorder is indeed a language

impairment (as suggested by Bernstein Ratner, 1997, among others), or, rather, a motor impairment that manifests primarily in speech production, possibly due to the complexity of motor coordination required (Max, Guenther, Gracco, Ghosh, & Wallace, 2004; Namasivayam & van Lieshout, 2011). The

* Corresponding authors. The Gonda Multidisciplinary Brain Research Center, Bar-Ilan University, Ramat-Gan 5290002, Israel.

E-mail addresses: vered.kronfeld@gmail.com (V. Kronfeld-Duenias), michalb@mail.biu.ac.il (M. Ben-Shachar).

<http://dx.doi.org/10.1016/j.cortex.2016.04.001>

0010-9452/© 2016 Elsevier Ltd. All rights reserved.

specific aspect of language processing affected in people who stutter is also subject for debate, with proposals ranging from motor-programming of speech acts to lexical retrieval, or even grammatical processing (see [Bloodstein & Ratner, 2008](#), chapter 8). Here, we contribute to this debate from a neuro-anatomical perspective, by examining which language stream is implicated in individuals who stutter.

Early models of language neuroanatomy suggested that the human language network consists of Broca's region, Wernicke's region and the connection between them, known as the arcuate fasciculus (AF) ([Catani & Mesulam, 2008](#); [Geschwind, 1970](#); [Price, 2000](#)). Since then, the field of neurobiology of language has evolved and it is now commonly held that processing and producing language relies on a wide network of cortical and subcortical regions, connected through multiple, sometimes parallel, white matter pathways ([Poeppel, Emmorey, Hickok, & Pylkkänen, 2012](#)). A predominant framework for explaining language processing in the brain suggests that, similarly to the visual and auditory systems, language is processed via two converging streams: a dorsal stream involved in mapping sound to articulation and a ventral stream involved in mapping sound to meaning ([Hickok & Poeppel, 2004, 2007](#); [Saur et al., 2008](#)). Adopting this dual stream model for language, our approach identifies the dorsal and ventral streams of the human language network in individuals who do and do not stutter, and compares their structural properties, aiming to identify the language stream implicated in persistent developmental stuttering.

In agreement with the view that language is processed in a wide network of brain regions, functional imaging studies of developmental stuttering have documented atypical patterns of activation in distributed brain regions, including right frontal regions, bilateral auditory cortex, motor regions, cerebellum and the basal ganglia (see [Alm, 2004](#); [Belyk, Kraft, & Brown, 2015](#); [Brown, Ingham, Ingham, Laird, & Fox, 2005](#)). Previous studies of white matter structures in persistent developmental stuttering have reported abnormalities in multiple white matter structures including white matter adjacent to bilateral inferior frontal gyrus, bilateral ventral premotor cortex, right superior temporal gyrus and in the corpus callosum ([Beal, Gracco, Brettschneider, Kroll, & De Nil, 2013](#); [Beal, Gracco, Lafaille, & Luc, 2007](#); [Cai et al., 2014](#); [Chang, Erickson, Ambrose, Hasegawa-Johnson, & Ludlow, 2008](#); [Choo, Chang, Zengin-Bolat kale, Ambrose, & Loucks, 2012](#); [Choo et al., 2011](#); [Connally, Ward, Howell, & Watkins, 2014](#); [Cykowski, Fox, Ingham, Ingham, & Robin, 2010](#); [Jäncke, Hänggi, & Steinmetz, 2004](#); [Sommer, Koch, Paulus, Weiller, & Büchel, 2002](#); [Watkins, Smith, Davis, & Howell, 2008](#)). However, the literature in this field shows little consistency with regards to the location of the implicated brain regions and the direction of the difference (for illustration of some of these inconsistencies, see Fig. 1 of [Cai et al., 2014](#)).

The most replicable finding in the study of white matter in adults and children who stutter comes from several whole brain voxel-based studies that indicate group-related reductions in fractional anisotropy (FA) within the white matter of the left Rolandic operculum (RO), located medially to Brodmann area 44 ([Chang et al., 2008](#); [Connally et al., 2014](#); [Cykowski et al., 2010](#); [Sommer et al., 2002](#); [Watkins et al., 2008](#)). The left RO is packed with long- and short-range

association fibers. Therefore, mapping this cluster into a specific pathway is particularly challenging. Fig. 1 illustrates this point by demonstrating fibers that pass through the left RO in a representative participant. The delineated tracts include the long (orange) and anterior (yellow) segments of the AF ([Catani, Jones, & Ffytche, 2005](#)), as well as several local tracts (dark red) connecting the ventral precentral cortex with the insula, pars triangularis and post central gyrus ([Catani et al., 2012](#)). Indeed, differences in the left RO were previously interpreted as indicating an abnormality in the dorsal language stream, specifically in the AF ([Chang et al., 2008](#); [Chang, Synnestvedt, Ostuni, & Ludlow, 2010](#); [Cykowski et al., 2010](#); [Watkins et al., 2008](#)), or as an impairment in shorter connections between sensorimotor cortex and the frontal operculum or ventral premotor cortex ([Sommer et al., 2002](#)). One recent study that used tractography to isolate individual tracts have shown differences in the bilateral AF in people who stutter ([Connally et al., 2014](#)), in support of the former interpretation. However, this analysis targeted the long segment of the AF specifically, without comparison to other segments of the dorsal stream or to the ventral stream.

To date, white matter studies have not yet reported significant stuttering-related differences in the ventral stream of adults who stutter (AWS¹). However, failing to find a significant group difference in voxel-based analyses could potentially be caused by registration errors, for example if the same tract of different individuals registers to different voxels in template space. Analyses using individualized tract identification may provide increased sensitivity (see [Ben-Shachar, Dougherty, & Wandell, 2007](#) for a detailed discussion). For example, we recently reported a difference in the frontal aslant tract (FAT) between AWS and controls ([Kronfeld-Duenias, Amir, Ezrati-Vinacour, Civier, & Ben-Shachar, 2016](#)), even though this difference had not been discovered in previous voxel-based group comparisons. Similarly, in studies of white matter pathways associated with reading abilities, early voxel-based studies identified dyslexia-related differences only in the dorsal pathways ([Deutsch et al., 2005](#); [Klingberg et al., 2000](#)). These findings have indeed been supported by later individualized tract based studies of reading associations in the AF ([Yeatman et al., 2011](#)). However, more recent individualized tract based studies have also recovered reading-related associations in the inferior longitudinal fasciculus ([Cummine et al., 2015](#); [Yeatman, Dougherty, Ben-Shachar, & Wandell, 2012](#)), which had not been discovered in previous voxel-based comparisons. We therefore suggest that a direct group comparison of microstructural properties using individualized tract identification is warranted in order to assess the contribution of the dorsal and ventral language pathways to persistent developmental stuttering. Based on the literature discussed above, we hypothesize that this approach will reveal differences in the microstructural properties of the dorsal, but not ventral, language stream.

In this study we use diffusion magnetic resonance imaging (MRI) and tractography to examine the microstructural and macrostructural properties of the dorsal and ventral language-related pathways in AWS and matched controls. We

¹ The term AWS refers to adults with persistent developmental stuttering, excluding cases of acquired stuttering.

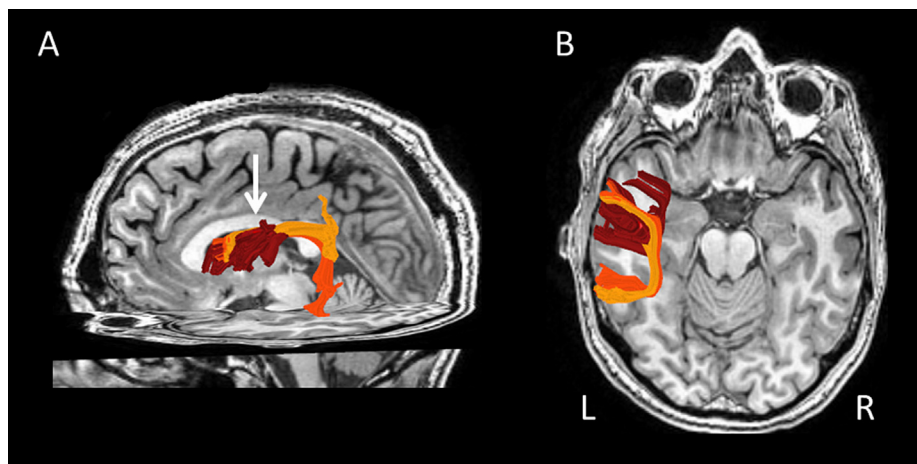


Fig. 1 – Long range and local fiber tracts passing through the left RO. Shown are tracts going through the left RO in a single participant (male, control). (A) Lateral view from the left, tracts are shown against the background of a midsagittal T1; (B) View from the top, tracts are shown with an axial T1 background. Fiber tracking was initialized from the entire left hemisphere and the resulting fibers were intersected (using a logical AND operation) with a 5 mm-radius sphere placed in the left RO (marked with a white arrow). The sphere was centered around the Montreal neurological institute (MNI) coordinate $[-42, -9, 25]$ following [Chang et al. \(2008\)](#). The delineated tracts include the long segment of the AF (orange), the anterior segment of the AF (yellow) and several local tracts (dark red) connecting the ventral precentral cortex with the insula, pars triangularis and post central gyrus. Abbreviations: Rolandic Operculum (RO), Left (L), Right (R).

identify bilateral pathways belonging to the dorsal and ventral streams in each participant and compare microstructural (diffusivity) and macrostructural (volume) properties of the identified tracts between the groups. Further, we go beyond the global tract diffusivity estimates and compare the diffusivity profiles of each tract, which allows us to identify local differences in diffusivity along the tract. Our approach aims to identify selective group differences related to persistent developmental stuttering in adults, thereby extending the current knowledge of the involvement of the dorsal and ventral streams in the neural basis of this disorder, but also contributing to existing models of language and its typical production.

1. Materials and methods

1.1. Participants

A total of 34 individuals participated in this study. The participants were all native Hebrew speakers. They were physically healthy and reported no history of neurological disease or psychiatric disorder. Before participating, each participant signed a written informed consent according to protocols approved by the Helsinki committee of the Tel-Aviv Sourasky Medical Center and by the ethics committee of the Humanities Faculty in Bar-Ilan University.

Our sample is described in detail in [Kronfeld-Duenias et al. \(2016\)](#). For completeness, we reiterate here the relevant details related to participant selection and group assignment. Participants were assigned to the group of AWS based on the following criteria: (a) reported a history of stuttering since childhood, (b) exhibited a minimum of three stuttering-like disfluencies (SLD; [Ambrose & Yairi, 1999](#)) per 100 syllables

during an unstructured interview (described below) and (c) scored a total of at least 10 on the Stuttering Severity Instrument (SSI-III; [Riley, 1994](#)). These inclusion and exclusion criteria were aimed to ensure that all AWS in our sample were adults with persistent developmental stuttering (i.e., developed stuttering from childhood without any known neurological damage). Assignment of participants to the control group was based on their self-report of having no history of stuttering.

To ensure that all participants assigned to the group of AWS were indeed individuals who stutter, two experienced speech pathologists (O.A. and R.E.) were asked to blindly confirm the original classification based on their impression from an audio-visual recording of an unstructured interview of the participants (described below). Classification was performed separately by each speech pathologist. Only those participants who were classified by both speech pathologists as individuals who stutter were assigned to the group of AWS. Based on these criteria, 15 participants were assigned to the group of AWS [mean age: 32 y, age range (19–52 y), three females]. 19 participants were assigned to the control group [mean age: 33 y, age range (19–53 y), three females]. [Table 1](#) presents the average demographic characteristics of the AWS and the control participants.

1.2. Assessment of stuttering frequency

To assess the frequency of stuttering, participants were evaluated during two speaking tasks: an unstructured interview and a reading task ([Riley, 1994](#)). In both tasks, each participant was seated in a quiet room together with one of the experimenters (V.K-D.). In the unstructured interview, participants were asked to talk for 10 min about a neutral topic, such as a recent travel experience, a movie or a book. In

Table 1 – Subject demographics and fluency measures^a.

	AWS (N = 15)	Controls (N = 19)	p
Age (years)	31.733 (9.93)	33.26 (9.91)	n.s
Gender	12M/3F	16M/3F	n.s
Handedness ^b	96 (8.28)	89.63 (17.84)	n.s
Education (years)	14.7 (2.86) ^c	15.31 (2.8)	n.s
SLD (%)	12.36 (16.73)	2.17 (1.03)	*p = .012
St. Syll. (%)	7.86 (3.95)	2.1 (.99)	*p = 7.1 × 10 ⁻⁷

*p < .05.

Abbreviations: Adults who stutter (AWS), stuttering-like-disfluencies (SLD) per 100 syllables, Stuttered syllables (St. Syll.), not significant (n.s), male (M), female (F).

^a Mean values and standard deviations (in parentheses) are shown for the AWS and control participants.

^b Handedness scores are based on the Edinburgh handedness inventory (Oldfield, 1971). 100 indicates full right handedness, -100 indicates full left handedness.

^c Education data are missing in two AWS, N = 13.

the reading task, each participant was asked to read aloud one of three paragraphs from the standardized and phonetically balanced Thousand Islands reading passage (Amir & Levine-Yundof, 2013). The three paragraphs were of similar length (on average: 200 syllables) and the different paragraphs were assigned to the participants in a random order. Both tasks were recorded using a digital video camera (Sony DCR-DVD 106E, Sony Corporation of America, New York, NY) with a noise canceling microphone (Sennheiser PC21, Sennheiser Electronic Corporation, Berlin, Germany). Audio signals of the unstructured interview were digitally recorded using audio processing software (Goldwave, Inc., St. John's, Canada), on a mono channel, with a sampling rate of 48 kHz (16 bit).

Based on the data recorded during the two speaking tasks, percentage of SLDs was calculated as the relative number of part-word repetitions, monosyllabic-word repetitions and dysrhythmic phonations (Ambrose & Yairi, 1999). Percent of stuttered syllables, stuttering duration scores and physical concomitants were further evaluated to obtain stuttering severity scores for AWS, according to the SSI-III (Riley, 1994).

1.3. Image acquisition

MRI was performed on a 3T General Electric MRI scanner at the Tel-Aviv Sourasky Medical Center. The MRI protocol included standard anatomical and diffusion imaging sequences, acquired with an eight channel head-coil. Participants were asked to lie still during the scan, and their head motion was minimized by placing cushions around their heads. Functional MRI experiments were also included in the scan protocol but those data are reported elsewhere (Halag-Milo et al., 2016).

T1 image acquisition: High resolution T1 weighted anatomical images were acquired using a 3D fast spoiled gradient echo (FSPGR) sequence. We collected about 150 axial slices (± 12 slices), covering the entire cerebrum, with a spatial resolution of $1 \times 1 \times 1$ mm voxel size.

Diffusion weighted image acquisition: A standard diffusion tensor imaging (DTI) protocol was applied by means of a single-shot spin-echo diffusion-weighted echo-planar imaging (DW-EPI) sequence. We collected ~68 axial slices, adjusting

the number of slices to cover the entire cerebrum in each participant (240 mm field of view; 128×128 matrix; 2 mm thick axial slices; voxel size: $\sim 2 \times 2 \times 2$ mm). 19 diffusion-weighted volumes ($b = 1000$ sec/mm²) and one reference volume ($b = 0$ sec/mm²) were acquired using a standard direction matrix (e.g., Kronfeld-Duenias et al., 2016; Sasson, Doniger, Pasternak, & Assaf, 2010; Sasson, Doniger, Pasternak, Tarrasch, & Assaf, 2012, 2013). This protocol was repeated twice to achieve improved signal-to-noise ratio. Scan repetitions were not averaged so that tensors were fit to the entire dataset from both scans (see Data preprocessing). Scanning 19 directions twice was motivated by the fact that short scan time (5:50 min per scan) reduces the chances of within-scan motion while maintaining robust anisotropy measurements (Jones, 2004). While a 19 direction protocol has its limitations (see Discussion), it has been used successfully in many recent studies that use the tensor model (Hofstetter, Tavor, Tzur-Moryosef, & Assaf, 2013; Tavor et al., 2014).

1.4. Software

Data preprocessing and tractography analyses were performed using Matlab 2012b (The Mathworks, Natick, MA). For data preprocessing we used the 'mrDiffusion' package (<http://web.stanford.edu/group/vista/cgi-bin/wiki/index.php/MrDiffusion>), the Automated Fiber Quantification (AFQ) package (Yeatman, Dougherty, Myall, Wandell, & Feldman, 2012) and functions from SPM5 (Friston & Ashburner, 2004). Visual inspection of the tracts and manual cleaning were performed with 'Quench', an interactive 3D visualization tool (Akers, 2006). Statistical analyses were conducted using STATISTICA version 12 and SPSS Version 21.

1.5. Data preprocessing

As a first step, T1 images were aligned to the anterior and posterior commissures (AC–PC) orientation. Diffusion weighted images were corrected for Eddy-current distortions and head motion (Rohde, Barnett, Basser, Marengo, & Pierpaoli, 2004). Each diffusion weighted image was registered to the mean of the two non-diffusion weighted (b_0) images and the mean b_0 image was registered automatically to the T1 image, using a rigid body mutual information maximization algorithm. Then, the combined transform resulting from motion correction, Eddy-current correction and anatomical alignment was applied to the raw diffusion data once, and the data were resampled at exactly $2 \times 2 \times 2$ mm isotropic voxels. By applying the combined transform we achieved AC–PC aligned T1 registered images while only resampling the raw data once. Next, the table of gradient directions was appropriately adjusted to fit the resampled diffusion data (Leemans & Jones, 2009).

We fitted the raw diffusion data with the tensor model using a standard least-squares algorithm. Then we extracted the eigenvectors and eigenvalues of the tensor and calculated FA as the normalized standard deviation of the eigenvalues (Basser & Pierpaoli, 1996). Using the eigenvalues we also calculated mean diffusivity (MD) as the average of all three eigenvalues. In addition, axial diffusivity (AD) and radial diffusivity (RD) were calculated in regions that showed significant FA difference between the groups. AD and RD were defined as the diffusivity

along the principal axis and as the average diffusivity along the two remaining secondary axes, respectively.

1.6. Tract identification protocol

Adopting the dual stream architecture (Hickok & Poeppel, 2004, 2007; Saur et al., 2008), we identified two dorsal and two ventral language pathways in each participant's left and right hemispheres. Dorsally, we identified the long and anterior segments of the AF (Catani et al., 2005). In subsequent figures we refer to these tracts as AF_{long} and AF_{ant} , respectively. Ventrally, we identified the inferior fronto-occipital fasciculus (IFOF) and the uncinate fasciculus (UNC) (Friederici, 2009; Saur et al., 2008). Fig. 2 shows the set of four tracts identified in the left hemisphere of a single participant (right hemisphere tracts not shown).

To identify the tracts we used the following three steps (demonstrated in Fig. 3):

Step 1 – Whole brain fiber tractography: Whole brain fibers were tracked in the native space of each participant using a deterministic streamlines tracking algorithm (Basser, Pajevic,

Pierpaoli, Duda, & Aldroubi, 2000; Mori, Crain, Chacko, & Van Zijl, 1999) with a fourth-order Runge–Kutta path integration method (1 mm fixed step size, eight seed points per voxel). The tracking algorithm was seeded with a white matter mask of all voxels with FA greater than .2 and tracking was halted when FA dropped below .15 or if the angle between the last and the next step direction was greater than 30° (Dougherty et al., 2007). Minimum streamline length was set to 20 mm.

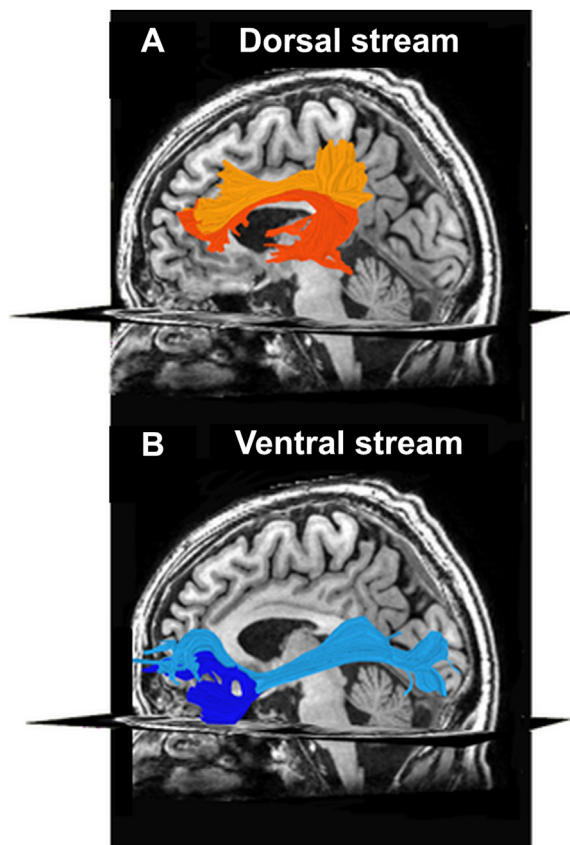


Fig. 2 – Dorsal and ventral tracts of interest. Shown are the left hemisphere dorsal (A) and ventral (B) tracts identified in a single participant (male, AWS group). The tracts are overlaid on sagittal T1 images. The identified tracts include the long segment of the AF (orange), the anterior segment of the AF (yellow), IFOF (light blue), UNC (dark blue). These tracts were identified bilaterally in each participant but only left tracts are visualized here.

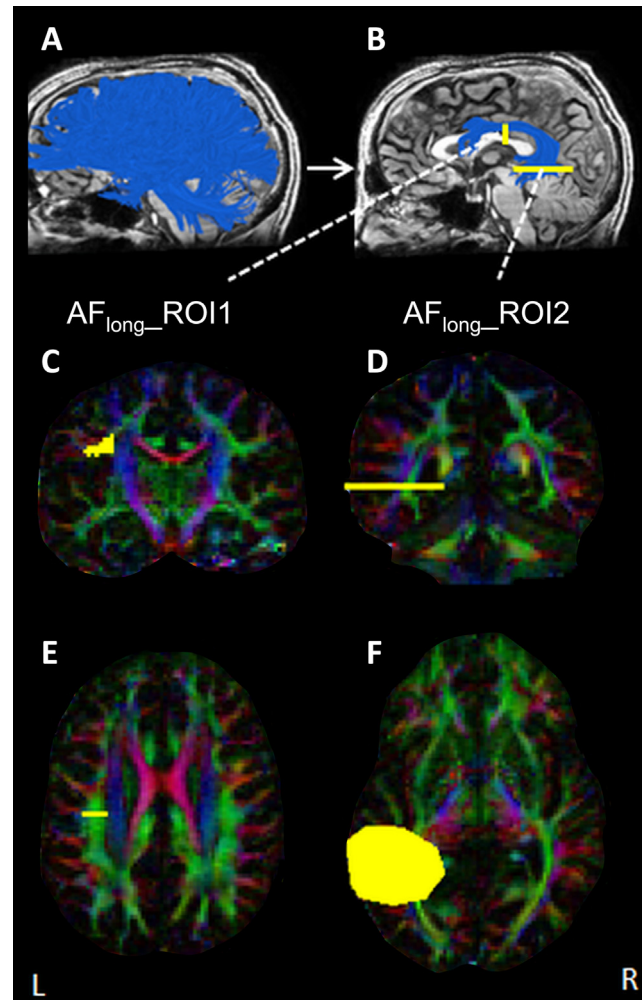


Fig. 3 – Tract identification. Steps 1 and 2 of the tract identification process are demonstrated for a single tract, the left long segment of the AF, in a single participant (male, AWS group). (A) Fiber tracking from the white matter mask of the entire brain generates a large set of virtual fibers (Step 1, shown in blue). (B) The global fiber group is intersected with two ROIs (shown in yellow), generating a restricted fiber group (Step 2). The locations of AF_{long_ROI1} and AF_{long_ROI2} are shown on coronal (C–D) and axial (E–F) color-coded maps that encode the PDD in each voxel. Voxels with a PDD along the left–right axis are shown in red, anterior–posterior PDD in green, inferior–superior PDD in blue. For further information on the locations of the ROIs used for the identification of other tracts of interest, see [Methods](#) and [Fig. S1](#). Abbreviations: long segment of the Arcuate Fasciculus (AF_{long}), Region Of Interest (ROI).

Step 2 – Tract delineation: We used a multiple regions of interest (ROIs) approach to identify the tracts in each participant's data. Anatomically defined ROIs were placed in each participant's native space and the fibers tracked from the entire brain (Step 1) were intersected with these ROIs. The ROIs used for the identification of the long segment of the AF, IFOF and UNC were drawn according to a published protocol (Wakana et al., 2007). The ROIs for the identification of the anterior segment of the AF, which was not explicitly described in that paper, were adapted from the protocol for finding the superior longitudinal fasciculus and the AF, with slight modifications made to the logical AND/NOT operations performed during the identification process. All ROIs were manually drawn on individual color-coded maps that encode the principal diffusion direction (PDD) in each voxel. Below we provide a short description of the ROIs used for the identification of each tract (see [Supplemental Fig. S1](#) for a demonstration of the ROIs in a single participant). The same guidelines were applied separately for identifying the left and right tracts, but they are described here only once.

To identify the long segment of the AF ([Fig. S1A](#), see also [Fig. 3](#)), we identified a coronal slice that passes through the middle of the posterior limb of the internal capsule. On it we drew a frontal green (anterior-posterior PDD) triangle that served as the frontal ROI (AF_{long}-ROI1). A second, temporal ROI was placed on an axial slice at the level of the anterior commissure (AF_{long}-ROI2). Fibers tracked in Step 1 were intersected with both ROIs sequentially (ROI1 was always intersected first for all the tracts).

To identify the anterior segment of the AF, we used the frontal AF_{long}-ROI1 (now named AF_{ant}-ROI1) and a parietal ROI covering the entire coronal plane at the level of the posterior edge of the splenium of the corpus callosum (AF_{ant}-ROI2). Fibers tracked in Step 1 were intersected with both ROIs sequentially. We then excluded fibers with temporal endpoints by applying a logical NOT operation with AF_{long}-ROI2 (named here AF_{ant}-ROI3). See [Fig. S1B](#) for visualization.

To identify the IFOF, a frontal ROI was drawn on a coronal slice at the anterior edge of the genu of the corpus callosum (IFOF-ROI1). An occipital ROI was identified in a coronal slice at the middle point between the posterior edge of the cingulum and the posterior edge of the parieto-occipital sulcus (IFOF-ROI2). See [Fig. S1C](#) for visualization.

To delineate the UNC, we identified the most posterior coronal slice in which the temporal lobe is separated from the frontal lobe. On this slice we drew a temporal ROI (UNC-ROI2) and a frontal ROI (UNC-ROI1). See [Fig. S1D](#) for visualization.

Step 3 – Fiber tract cleaning: To remove outlier tracts, we used an automated cleaning procedure that removed fibers extending over four standard deviations from the mean fiber length or spatially deviating more than five standard deviations from the core of the tract (see [Yeatman, Dougherty, Myall, et al., 2012](#) for further details). Next, we manually inspected all the tracts in each individual using a gesture based interface ('Quench', see [Software](#)) and excluded single fibers that clearly did not fit the tract definition. For example, we removed tracts that touched or crossed the midsagittal plane.

To verify that the manual cleaning phase did not introduce any systematic group differences, we compared the percentage of cleaned fibers between the groups. Specifically, we calculated the individual exclusion ratios per tract as [the number of streamlines that were manually excluded from each tract] divided by [the number of streamlines in the original tract before cleaning]. Next, we compared the exclusion ratios between the groups using two-tailed t-tests with unequal variance.

1.7. Volume and whole tract diffusivity measures

We estimated the volume of each tract for each participant as the number of voxels visited by the reconstructed streamlines. To control for overall differences in brain size, we divided the tract volume estimates by the volume of the white matter in the entire brain (defined as the number of voxels with FA > .2). The result was then multiplied by 100 to obtain a normalized tract volume score (in percentages) for each tract in each participant. In addition to the volume estimates, we calculated the average FA and average MD across all voxels visited by the tract (tract-FA and tract-MD, respectively).

To assess group differences in these three dependent measures, we conducted three separate mixed design analyses of variance (ANOVAs) with Group (AWS/controls) as between-subject factor and Stream (dorsal/ventral), Hemisphere (left/right) and Tract (two tracts within each stream) as within-subject factors. Significant Group-related interactions were followed up with Tukey's honest significant difference (HSD) test to identify the pairwise comparison that caused the significant group-related interaction. Significant Stream effects identified in this way were followed up with two-tailed t-tests comparing the groups separately in the left stream and in the right stream (two comparisons, Bonferroni corrected). To this end, measures of the left stream were calculated by merging the two tracts that compose the left stream (the left long and anterior segments of the AF) and measures of the right stream were calculated separately on the tracts that compose the right stream (shared voxels were counted only once in each hemisphere).

To examine the stability of these results and assess the likelihood that they have been driven by extreme values, 95% confidence intervals were calculated on the differences between group means, using a bootstrap analysis with 10,000 iterations ([Efron & Tibshirani, 1993](#)). Finally, significant effects detected in the ANOVAs described above were followed up with an analysis of covariance (ANCOVA) to evaluate the contribution of age (added to the analysis as a covariate).

1.8. FA and MD profiles along the tract

FA and MD profiles of each tract were obtained by sampling the tract at 100 equi-spaced nodes (defined between the first and second ROIs used for tract identification) and calculating FA and MD in each node as a weighted average across the streamlines of that tract ([Yeatman, Dougherty, Myall, et al., 2012](#)). FA and MD profiles were compared between the groups using multiple two-tailed t-tests for independent samples. A permutation-based multiple comparisons

correction (Nichols & Holmes, 2002) was used to calculate the critical cluster size of adjacent significant t-tests. Significance was corrected for 800 comparisons (8 tracts \times 100 nodes in each tract) setting the corrected alpha to .05.

We report clusters of nodes in which (1) all neighboring nodes significantly differed between the groups at a level of .05 (uncorrected) and (2) the cluster of significant values [detected in (1)] was larger than the critical cluster size (Nichols & Holmes, 2002; Yeatman, Dougherty, Myall, et al., 2012). In such clusters, we evaluated the source of the significant difference in FA by calculating AD and RD values and comparing them between the groups using two-tailed t-tests (significance corrected for two comparisons using a Bonferroni correction). To examine if the difference in FA, AD and RD values could be driven by a few extreme values, 95% confidence intervals were calculated on the difference between the group means using a bootstrap analysis with 10,000 iterations (Efron & Tibshirani, 1993).

2. Results

2.1. Behavioral results

Participants in the group of AWS scored an average SSI score of 24.07 [standard deviation: 7.38; range (10–41.5)]. The wide range of SSI scores demonstrated that this group consisted of different degrees of symptoms, ranging from very mild to very severe. The clinical evaluation of speech fluency measures verified a significant group difference between AWS and fluent controls in measures of speech fluency [SLD: $t(32) = 2.66$, $p < .05$; percent of stuttered syllables: $t(32) = 6.14$, $p < 10^{-6}$; see Table 1 for significance levels]. The groups did not differ in age, handedness or education levels.

2.2. Tract identification

We identified the left long segment of the AF, bilateral anterior segment of the AF, bilateral IFOF and bilateral UNC in all participants ($N = 34$). The right long segment of the AF was successfully identified in 28 of the 34 participants, but could not be traced in six participants (three of each group) (see Catani et al., 2007; Lebel & Beaulieu, 2009; Wahl et al., 2010 for similar findings). Missing the right long segment of the AF is a common finding when using deterministic tractography and does not imply the inexistence of this tract in these participants (Yeatman et al., 2011), but rather, reflects the shortcomings of deterministic tractography. Fig. S2 shows the mean exclusion ratios for each tract and each group, verifying that there were no significant group differences in the percentage of fibers excluded during the manual cleaning phase (Fig. S2, $p > .05$).

The missing values in the right long segment of the AF were handled as follows: In the volume analysis, missing data points were coded as zero volume. In the diffusivity analyses we replaced the missing data points with the average FA or MD values of the relevant group. We further validated that the results of the volume analysis did not result from the zero-

replacement by repeating the analysis while replacing missing data points with group-average normalized volumes.

2.3. Left dorsal tracts are smaller in AWS

To assess group differences in tract volume, we conducted a mixed design ANOVA with Group as a between-subject factor and Stream, Hemisphere and Tract as within-subject factors. Normalized volume was the dependent variable. This analysis

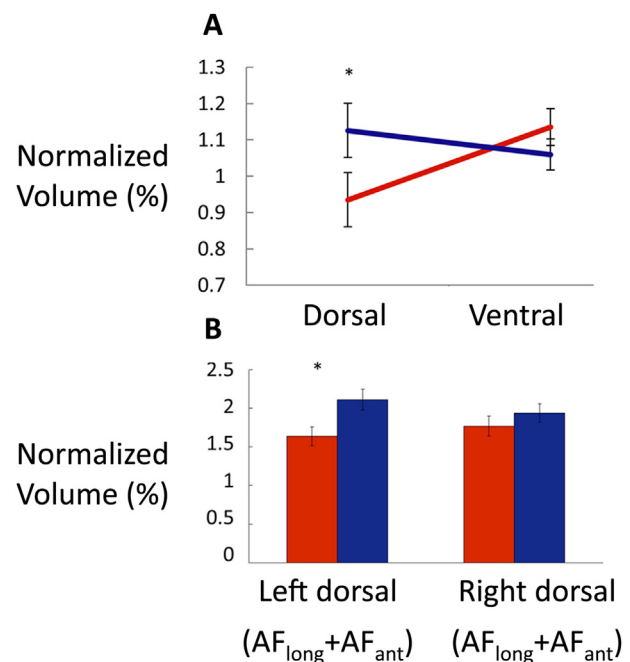


Fig. 4 – Group comparison of tract volumes. (A) This panel illustrates the significant Group by Stream interaction found in the ANOVA performed over tract volumes [$F(1,32) = 7.8$, $p < .05$]. Mean normalized volume estimates of the dorsal and ventral streams (averaged across both tracts within a stream and across both hemispheres for each stream) are shown for AWS (red) and controls (blue). Error bars represent ± 1 standard error of the mean. Post hoc comparisons (calculated with Tukey's HSD test, see text) showed that the interaction stems from a significant group difference in the dorsal, not ventral, stream, as indicated by the asterisk. **(B)** Zooming in on the dorsal tracts only, this panel illustrates the combined volume of the dorsal tracts in each hemisphere separately, in AWS (red) and controls (blue). A significant group difference is observed in the combined volume of the left dorsal tracts ($p < .05$, Bonferroni corrected for two comparisons, indicated by an asterisk) but not in the right dorsal tracts ($p > .3$). The range on the y-axis is different between the panels because the values in A represent the average volumes of single tracts (which are the values that were tested in the ANOVA), while the values in B represent the combined volume of the merged long and anterior segments of the AF (see Methods). Abbreviations: long segment of the Arcuate Fasciculus (AF_{long}), anterior segment of the Arcuate Fasciculus (AF_{ant}).

revealed a significant Group by Stream interaction [$F(1,32) = 7.8, p < .01$, illustrated in Fig. 4A] and a significant Group by Hemisphere interaction [$F(1,32) = 4.38, p < .05$]. A significant main effect of Hemisphere was also evident across the two groups [$F(1,32) = 10.56, p < .01$]. Table 2 lists F values and significance levels for this ANOVA.

We repeated this ANOVA while replacing the six missing data points (i.e., participants with no detected right long segment, three in each group) with group-averaged normalized volumes. The results replicated the original analysis, showing a significant Group by Stream interaction [$F(1,32) = 7.4, p = .01$], a significant Group by Hemisphere interaction [$F(1,32) = 5.35, p = .02$] and a significant main effect of Hemisphere [$F(1,32) = 7.69, p = .009$]. An ANCOVA analysis with age as covariate replicated the same interactions, showing a significant Group by Stream interaction [$F(1,31) = 7.47, p = .01$] as well as a marginally significant Group by Hemisphere interaction [$F(1,31) = 4.14, p = .05$].

To further interpret the significant Group by Stream interaction we conducted post hoc comparisons using Tukey's HSD test (corrected alpha set at $p < .05$). This analysis revealed that the volume estimates of the dorsal stream were significantly smaller in AWS compared with controls ($p = .05$), while the volume estimates of the ventral stream did not differ significantly between the groups ($p > .3$, see Fig. 4A). We further evaluated the source of the difference in the dorsal stream, by conducting group comparisons of the dorsal stream volumes, separately in each hemisphere (Fig. 4B). A significant group difference was found in the left dorsal stream, but not in the right dorsal stream ($p < .05$, Bonferroni corrected for two comparisons). Specifically, AWS showed reduced volumes in the left dorsal stream compared with controls [$t(32) = 2.52, p = .02$], but this was not the case in right dorsal stream that showed no significant group differences in volume ($p > .3$). Confidence intervals calculated on the difference between the group means confirmed that the group difference in the volume of the left dorsal stream was larger than zero at 95% confidence [$CI_{95\%} = (.13, .83)$] but not so for the right dorsal stream [$CI_{95\%} = (-.16, .5)$]. The latter analysis confirms that the difference in the volume of the left dorsal stream is unlikely to be driven by a few extreme cases. Thus, we conclude that the significant group difference observed in the volumes of the dorsal stream is derived from smaller volumes of the left dorsal tracts.

Table 2 – Normalized tract volume – ANOVA results^a.

	MS	F	p
Group	.2224	1.126	.297
Stream	.3066	2.012	.166
Hemisphere	.7037	10.564	.003*
Group × Stream	1.877	7.796	.009*
Group × Hemisphere	.2915	4.376	.044*
Stream × Hemisphere	.0622	.649	.426
Group × Stream × Hemisphere	.0607	.633	.432

* $p < .05$.

^a For simplicity, effects involving Tract are not shown. Such effects are expected because of the overall difference in the size of different tracts, but are of no relevance to the current study.

2.4. AWS have lower FA in the right anterior segment of the AF

To assess overall group differences in FA of the dorsal and ventral tracts in AWS compared to controls, we conducted a mixed design ANOVA similar to the one described above, but now with mean tract-FA as the dependent variable. FA was averaged across the voxels visited by each tract, in each participant. These mean tract-FA estimates were entered into a mixed design ANOVA, with Group as a between-subject factor and Stream, Hemisphere and Tract as within-subject factors. This analysis did not detect a significant main effect of Group [$F(1,32) = .24, p = .62$], nor any significant group-related interaction [Group by Stream: $F(1,32) = 2.73, p = .1$; Group by Hemisphere: $F(1,32) = 3.88, p > .05$]. Fig. S3 shows mean tract-FA values in each group for each tract.

Averaging FA across the tract is prone to wipe out subtle differences in anisotropy between the groups, especially in long range fiber tracts such as the AF that demonstrate an overwhelming variability in FA values measured at different points along the tract (De Santis, Drakesmith, Bells, Assaf, & Jones, 2014; Yeatman et al., 2011). An alternative method, which we and others have used fruitfully in recent studies of typically and atypically developmental populations (Johnson et al., 2014; Kronfeld-Duenias et al., 2016; Travis, Leitner, Feldman, & Ben-Shachar, 2014) consists of analyzing tract profiles, where the dependent measure is not the mean tract-FA but rather local FA estimates at multiple locations along the tract. We applied this method here in order to examine whether subtle group differences do occur in specific locations along the dorsal or ventral tracts of AWS versus controls.

To this end, we calculated anisotropy profiles for each of the tracts and compared the profiles between the two groups (see Methods). Fig. 5 shows group FA profiles along the left (A, C) and right (B, D) dorsal tracts. Significant group differences were found in the right anterior segment of the AF (Fig. 5B, nodes 36–68, $p < .05$, family-wise-error correction for 800 comparisons along eight tracts and 100 nodes per tract). No significant differences were found in the left dorsal tracts (Fig. 5A, C), in the right long segment of the AF (Fig. 5D) or in any of the ventral tracts in either hemisphere (Fig. 6).

To further clarify the sources of FA reduction in the right anterior segment of the AF, we compared the axial and radial diffusivities in the same nodes where FA significantly differed between the groups. Significant group differences were found in both AD and RD measures ($p < .05$, Bonferroni corrected for two comparisons). As shown in Fig. 7, AWS showed a significant reduction in AD compared with controls [$t(32) = 2.43, p = .02$], as well as a significant elevation in RD [$t(32) = 2.7, p = .01$]. Confidence interval calculations applied to the differences between group means confirmed that the group differences were larger than zero at 95% confidence, for both FA [$CI_{95\%} = (.02, .11)$], AD [$CI_{95\%} = (.01, .06)$] and RD [$CI_{95\%} = (.01, .08)$] in nodes 36–68 of the right anterior segment of the AF. This analysis confirmed that the effects reported above are unlikely to be driven by a few extreme cases. Thus, we conclude that the significant reduction in FA values observed within the right anterior segment of the AF in AWS stemmed from both AD reduction and RD elevation in the group of AWS, compared with controls.

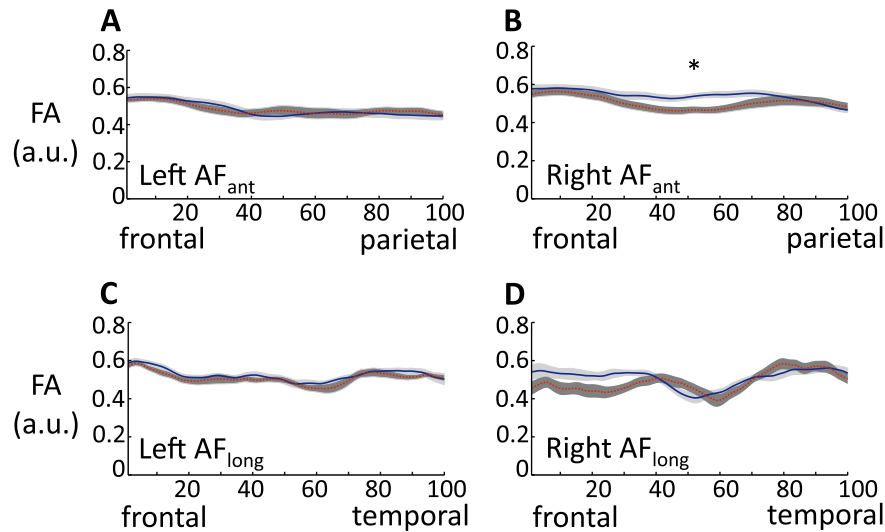


Fig. 5 – FA tract profiles, dorsal stream. Group-averaged FA profiles are plotted along left and right anterior segment of the AF (A–B) and along the left and right (C–D) long segment of the AF. The data are shown for AWS (red) and control participants (blue) with gray regions representing ± 1 standard error of the mean. Significant between-group differences are found in the right anterior segment of the AF (nodes 36–68, marked with *, $p < .05$, corrected). Abbreviations: Fractional Anisotropy (FA), arbitrary units (a.u.), long segment of the Arcuate Fasciculus (AF_{long}), anterior segment of the Arcuate Fasciculus (AF_{ant}).

2.5. No difference in MD values of dorsal and ventral tracts in AWS and controls

Similarly to the analysis of tract-FA, tract-MD measurements were entered into a mixed design ANOVA (see [Methods](#)). This analysis showed no main effect of Group [$F(1,32) = 2.08, p > .1$] nor any significant Group-related interaction [Group by Stream: $F(1,32) = .06, p > .8$; Group by Hemisphere: $F(1,32) = .21, p > .2$; see [Fig. S4](#) for group means]. An analysis of MD profiles (parallel to the one described above for FA profiles) did not

reveal any significant differences in MD values along the dorsal or ventral tracts ([Figs. S5 and S6](#)).

3. Discussion

Using an individualized tractography-based approach, we found differences in dorsal, but not in ventral, language-related tracts, in AWS compared to matched controls. Within the dorsal pathways, differences were observed in

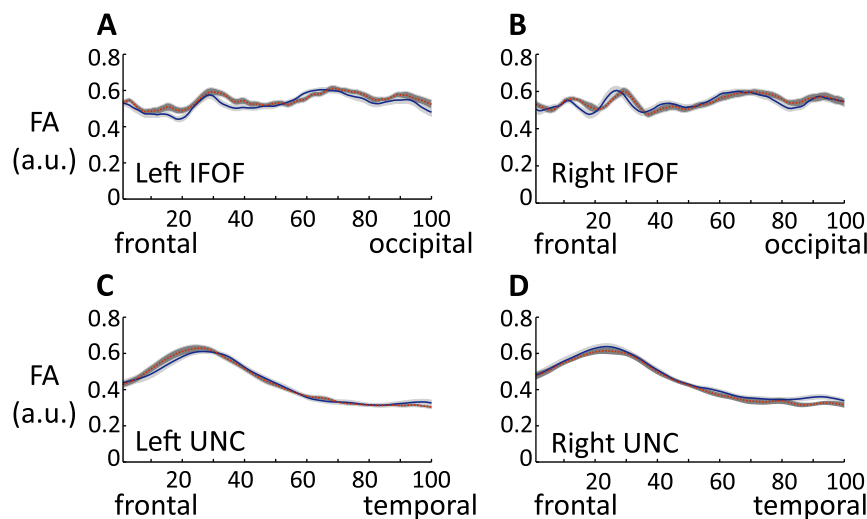


Fig. 6 – FA tract profiles, ventral stream. Group-averaged FA profiles are plotted along the left and right IFOF (A–B) and along the left and right UNC (C–D). The data are shown for AWS (red) and control participants (blue) with gray regions representing ± 1 standard error of the mean. Unlike in the dorsal stream ([Fig. 5](#)) no significant group differences are observed in any of the tracts. Abbreviations: Fractional Anisotropy (FA), arbitrary units (a.u.), Inferior Fronto Occipital Fasciculus (IFOF), Uncinate Fasciculus (UNC).

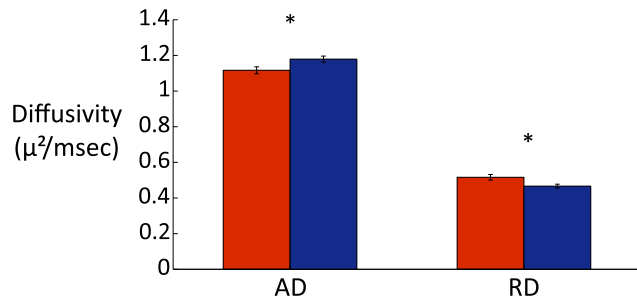


Fig. 7 – Group comparison of axial and radial diffusivities in regions that show a significant difference in FA. Bars indicate axial and radial diffusivities averaged across the nodes that show a significant group difference in the comparison of FA profiles (nodes 36–68, see Fig. 5). The diffusivities are shown in AWS (red) and in controls (blue), with error bars representing ± 1 standard error of the mean. Abbreviations: Axial diffusivity (AD), Radial diffusivity (RD), millisecond (msec). * denotes differences at the level of $p < .05$, corrected.

macrostructural and microstructural measures, and across both hemispheres: reduced volume was found in the left dorsal stream of AWS, and reduced anisotropy was found in the right dorsal stream of AWS.

The involvement of both hemispheres in the etiology of stuttering has long been proposed. In the 1920's it was widely accepted that many people who stutter are left-handers or ambidextrous who were forced to shift to right handedness by their parents and caregivers (Kushner, 2012). The Orton–Travis hypothesis, a dominant model of stuttering at the time, proposed that stuttering resulted from a failure of one hemisphere to become dominant over the other hemisphere (Travis, 1931). Many recent functional imaging studies indicate the involvement of both hemispheres in developmental stuttering (Belyk et al., 2015; Biermann-Ruben, Salmelin, & Schnitzler, 2005; Chang, Kenney, Loucks, & Ludlow, 2009; Kell et al., 2009; Lu et al., 2010; Watkins et al., 2008; Xuan et al., 2012). Structural white matter imaging studies indirectly support this idea by indicating micro- and macrostructural differences in the corpus callosum of individuals who stutter (Beal et al., 2013; Cai et al., 2014; Choo et al., 2011, 2012; Civier, Kronfeld-Duenias, Amir, Ezrati-Vinacour, & Ben-Shachar, 2015; Cykowski et al., 2010). In line with these results, our findings emphasize the role of both hemispheres in persistent developmental stuttering.

In contrast with the bilateral functional picture described above, previous DTI studies have, for the most part, highlighted left frontal white matter abnormalities as the core deficit in stuttering. Specifically, several diffusion weighted imaging studies of developmental stuttering indicated FA reductions in left frontal regions, in the vicinity of the left RO (Chang et al., 2008; Cykowski et al., 2010; Sommer et al., 2002; Watkins et al., 2008). In contrast with our hypothesis, which was based on these prior studies, we did not find FA differences in the left dorsal language tracts. This further contrasts with the common interpretation of previously reported voxel-based FA reductions in the left RO as an indication of an

abnormality in fronto-temporal connections via the AF (Cai et al., 2014; Chang et al., 2008; Chang, Horwitz, Ostuni, Reynolds, & Ludlow, 2011; Chang et al., 2010; Cykowski et al., 2010; Watkins et al., 2008). The fact that we found volume differences in the left dorsal tracts with no accompanying microstructural differences in these pathways can be related to previous reports of reductions in gray matter density (Beal et al., 2013; Kell et al., 2009) or cortical thickness (Lu et al., 2012) in the left inferior frontal gyrus of people who stutter. We propose that a smaller population of neurons in the left inferior frontal gyrus could be sending a smaller number of axons posteriorly through these tracts. Alternatively, the left dorsal tracts in AWS might not reach all the endpoints that it does in fluent controls, yielding a difference in the number of voxels covered by these tracts. The latter interpretation predicts that people who stutter will show less distributed activation patterns in cortical territories connected by the left dorsal tracts.

We suggest that previous reports of stuttering-related FA reductions in the left RO and the volume differences in the left dorsal stream found in this study may reflect different aspects of left frontal abnormalities. Under this assumption, previously recorded FA reductions in the left RO may reflect an impairment in a local, possibly motor–premotor tract (Max et al., 2004), or in cortico-striatal, motor-putamen projections (Civier, Bullock, Max, & Guenther, 2013) rather than an impairment in the left fronto-temporal/fronto-parietal connections which were traced here. Alternatively, if the left dorsal tracts are indeed smaller in AWS, as indicated by our results and by other tractography studies (Chang et al., 2011; Cieslak, Ingham, Ingham, & Grafton, 2015), then we might find coordinates in standard space that contain left dorsal fibers in controls but gray matter or short frontal U-shaped connections in AWS.² In such cases, voxel-based methods might detect microstructural differences between the different pathways sampled in each group, not within the same pathway sampled in both groups. The volume differences that we find here therefore provide a clear motivation for individualized tract identification as a method for defining white matter ROIs for the analysis of microstructural differences between AWS and controls.

Within the right hemisphere, our data point to FA reductions in the right anterior segment of the AF of AWS compared with fluent controls. Stuttering-related differences in diffusion properties of right hemisphere white matter regions were previously reported, but the results have been mixed with respect to the specific location and direction (reduction/elevation) of the reported differences. While several studies indicate FA elevations in white matter regions within the right hemisphere of stuttering individuals (Cai et al., 2014; Chang et al., 2008, 2010; Watkins et al., 2008), others indicate FA reductions in frontal and temporal regions in AWS versus controls (Cai et al., 2014; Watkins et al., 2008). The latter findings indicate FA reductions in white matter regions underlying the right superior temporal sulcus (Cai et al., 2014), as well as in white matter underlying pars

² For illustration of candidate short frontal connections, refer to Fig. 1; for a detailed description of short connections of the frontal lobe, see Catani et al. (2012).

orbitalis, posterior inferior frontal gyrus, precentral gyrus and ventral premotor cortex (Watkins et al., 2008). Notably, the FA reductions that we report are more posterior and medial relative to these frontal foci. They are located on the border of the frontal and parietal lobes, medially to the sensory-motor cortex involved in cortical control of articulation (Bouchard, Mesgarani, Johnson, & Chang, 2013; Brown et al., 2009). We propose that the FA reductions detected in the current study and in the abovementioned studies may reflect impairments at different locations along the right dorsal pathways. More research is necessary to determine whether the remaining inconsistencies in the literature on white matter in AWS are best explained in terms of the analysis methods used, the quality of the acquired data (e.g., motion, imaging protocol), or by differences in sample characteristics such as the distribution of age, stuttering symptoms and stuttering severity.

FA differences are notoriously hard to interpret in terms of differences in tissue properties, but it is important to be explicit about what may and may not be deduced from these findings. Based on the location of the detected FA differences at the core of the long range dorsal pathways, and given the relatively high anisotropy values in this cluster (over .4 in both groups), we can be fairly confident that we are probing differences in white matter tissue, and not, for example, differential partial voluming with gray matter. However, even within white matter, FA is affected by many factors, including axonal packing density, axonal diameter, myelination and directional coherence (Beaulieu, 2002). The FA reduction found in the right anterior segment of the AF of AWS may indicate a difference in any of these tissue properties. The finding that both increased RD and decreased AD accompany the FA differences that we report, suggests that AWS have larger water mobility in more than one direction (Jones, Knösche, & Turner, 2013). Previously, this pattern of results was reported in secondary Wallerian degeneration (Beaulieu, 2002; Burzynska et al., 2010), associated with axonal loss that is followed by increases in extracellular matrix. Future studies may take advantage of new quantitative imaging techniques in order to probe more directly the macromolecular content of white matter, thus getting us closer to a neurobiological interpretation of the differences found in stuttering (Assaf, Blumenfeld-Katzir, Yovel, & Basser, 2008; Mezer et al., 2013; Stikov et al., 2011).

Last, we return to the original question of whether developmental stuttering is a language deficit, and if so, which specific language systems are affected in stuttering. Our results clearly indicate differences in language-related tracts of AWS. However, our findings are bilateral, and restricted to the dorsal tracts, which are assumed to interface (directly or indirectly) between auditory and motor aspects of speech production (Hickok, 2012). We did not find any significant difference in the left ventral pathways which are thought to implement higher linguistic aspects such as language comprehension and lexical access (Hickok & Poeppel, 2007; Kümmerer et al., 2013; Saur et al., 2008). Moreover, in a recent publication we have examined specifically the contribution of pathways associated with more motor aspects of speech production in AWS, the FAT and the corticospinal tract (CST) (Kronfeld-Duenias et al., 2016). Our results show that microstructural properties of the left FAT differ between AWS

and controls, and predict speech fluency in AWS (but not in controls). The FAT (Catani et al., 2013), which connects the ventral inferior frontal cortex with the supplementary and pre-supplementary motor areas, is considered part of a “motor stream” in language (Dick, Bernal, & Tremblay, 2013). Its involvement in stuttering was further strengthened by a recent study that demonstrated stuttering following stimulation of the left FAT in patients who never suffered from stuttering prior to the operation (Kemerdere et al., 2016). Our findings do not rule out the possibility that stuttering may involve a language deficit. However, viewed in the context of the findings so far, our data provide neuroanatomical support for the view that stuttering involves an impairment in motor-control aspects of speech production, not an impairment in central, higher-level aspects of language processing.

3.1. Limitations

Our study is limited by several factors. First, the sample size is modest ($N = 15$ for AWS and $N = 19$ for controls), which reduces the statistical power of our analyses. It is possible that with larger samples we could demonstrate a significant difference even in mean tract-FA. For example, De Santis et al. (2014) show that around 20–25 participants are necessary to achieve a power of .9 at a relative effect size of 10% in group comparisons of mean tract-FA values within the AF (long and anterior segments), IFOF and UNC (see Fig. 9 of the cited paper). The fact that we could detect significant group differences (corrected for multiple comparisons) in local FA values along the right anterior segment of the AF suggests that the FA profile analysis may have reduced the variability and improved power. Still, using a larger sample would also have enabled subgrouping the individuals who stutter based on their stuttering severity scores (or based on other fluency measures). Such analyses are warranted in larger studies given the known immense variability in the manifestation and severity of stuttering symptoms.

Second, in this study we used a scan protocol with a limited angular resolution (19 diffusion directions). We chose this number of directions to shorten scan duration (5:50 min) in order to reduce the likelihood of within-scan head motion. We improved the signal-to-noise ratio by repeating the acquisition twice. While simulation studies recommend the use of at least 30 diffusion directions for the purpose of tractography (Jones, 2004), a recent study in human subjects demonstrated that similarly robust measurements are achieved using six and 30 directions in many white matter tracts delineated using deterministic tractography (Lebel, Benner, & Beaulieu, 2012). The authors of the latter study conclude that using repeated scans (as used here) along with at least six directions should be considered appropriate for the purposes of deterministic tractography.

Third, our results distinguish between the dorsal and ventral pathways, but are inconclusive in determining which of the two dorsal tracts (the long or the anterior segment of the AF) is implicated in developmental stuttering, since differences are detected in both tracts. The dorsal tracts share many voxels, and are therefore difficult to separate with any tractography method. Future studies may obtain better separation between these tracts using high-angular and spatial

resolution. Our findings using diffusion MRI are inherently limited to the structural level of analysis, and may not be used to evaluate directly the functional aspects affected in persistent developmental stuttering. A more direct assessment of the functional aspects related to the dorsal stream differences in persistent developmental stuttering may be achieved by future studies combining diffusion MRI with measurements of cortical functioning, e.g., functional MRI.

Finally, because all our participants were adults, our results cannot determine if the detected group differences constitute the cause for stuttering or reflect compensatory processes following years of stuttering. Previously, it has been suggested that the core deficit in stuttering is left hemispheric (Chang et al., 2008; Kell et al., 2009), and that the right hemisphere is over-activated to compensate for this deficit (Preibisch et al., 2003; but see Civier et al., 2015 for an alternative interpretation). The issue of cause and effect will be better addressed by longitudinal studies of at-risk children, starting before the age of stuttering onset, as well as by intervention studies in both children and adults, in which the neural correlates of behavioral improvement can be directly measured.

Acknowledgments

This work is supported by the Israel Science Foundation [513/11 to M.B.-S and O.A.], and by a Marie Curie International Reintegration Grant [DNLP 231029] awarded to M.B.-S. by the European Commission. V.K.D and O.C. were supported by the Israeli Center of Research Excellence in Cognition [I-CORE Program 51/11]. O.C. was supported by the Center for Absorption in Science, Ministry of Immigration Absorption, The State of Israel. The authors declare no competing financial interests. We thank the Israeli Stuttering Association (AMBI) for help with participant recruitment. We also thank the team at the Wohl institute for advanced imaging in Tel Aviv Sourasky Medical Center, for assistance with protocol setup and MRI scanning. We are grateful to Tali Halag-Milo for her assistance in data acquisition.

Supplementary material

Supplementary data related to this article can be found at <http://dx.doi.org/10.1016/j.cortex.2016.04.001>.

REFERENCES

Akers, D. (2006). CINCH: A cooperatively designed marking interface for 3D pathway selection. Paper presented at the User Interface Software and Technology meeting, Montreux, Switzerland.

Alm, P. A. (2004). Stuttering and the basal ganglia circuits: a critical review of possible relations. *Journal of Communication Disorders*, 37(4), 325–369.

Ambrose, N. G., & Yairi, E. (1999). Normative disfluency data for early childhood stuttering. *Journal of Speech, Language, and Hearing Research*, 42(4), 895–909.

Amir, O., & Levine-Yundof, R. (2013). Listeners' attitude toward people with dysphonia. *Journal of Voice*, 27(4), 524.e1–524.e10.

Assaf, Y., Blumenfeld-Katzir, T., Yovel, Y., & Basser, P. J. (2008). AxCaliber: a method for measuring axon diameter distribution from diffusion MRI. *Magnetic Resonance in Medicine*, 59(6), 1347–1354.

Basser, P. J., Pajevic, S., Pierpaoli, C., Duda, J., & Aldroubi, A. (2000). In vivo fiber tractography using DT-MRI data. *Magnetic Resonance in Medicine*, 44(4), 625–632.

Basser, P. J., & Pierpaoli, S. (1996). Microstructural and physiological features of tissues elucidated by quantitative diffusion tensor MRI. *Journal of Magnetic Resonance*, 111(3), 209–219.

Beal, D. S., Gracco, V. L., Brettschneider, J., Kroll, R. M., & De Nil, L. F. (2013). A voxel-based morphometry (VBM) analysis of regional grey and white matter volume abnormalities within the speech production network of children who stutter. *Cortex*, 49(8), 2151–2161.

Beal, D. S., Gracco, V. L., Lafaille, S. J., & Luc, F. (2007). Voxel-based morphometry of auditory and speech-related cortex in stutterers. *NeuroReport*, 18(12), 1257–1260.

Beaulieu, C. (2002). The basis of anisotropic water diffusion in the nervous system – a technical review. *NMR in Biomedicine*, 15(7–8), 435–455.

Belyk, M., Kraft, S. J., & Brown, S. (2015). Stuttering as a trait or state – an ALE meta-analysis of neuroimaging studies. *European Journal of Neuroscience*, 41(2), 275–284.

Ben-Shachar, M., Dougherty, R. F., & Wandell, B. A. (2007). White matter pathways in reading. *Current Opinion in Neurobiology*, 17(2), 258–270.

Bernstein Ratner, N. (1997). Stuttering: a psycholinguistic perspective. In R. F. Curlee, & G. M. Siegel (Eds.), *Nature and treatment of stuttering: New directions* (2nd ed., pp. 99–127). Boston, MA: Allyn & Bacon.

Biermann-Ruben, K., Salmelin, R., & Schnitzler, A. (2005). Right rolandic activation during speech perception in stutterers: a MEG study. *NeuroImage*, 25(3), 793–801.

Bloodstein, O., & Ratner, N. B. (2008). *A handbook on stuttering* (6th ed.). Stamford, CT: Delmar.

Bouchard, K. E., Mesgarani, N., Johnson, K., & Chang, E. F. (2013). Functional organization of human sensorimotor cortex for speech articulation. *Nature*, 495(7441), 327–332.

Brown, S., Ingham, R. J., Ingham, J. C., Laird, A. R., & Fox, P. T. (2005). Stuttered and fluent speech production: an ALE meta-analysis of functional neuroimaging studies. *Human Brain Mapping*, 25(1), 105–117.

Brown, S., Laird, A. R., Pfordresher, P. Q., Thelen, S. M., Turkeltaub, P., & Liotti, M. (2009). The somatotopy of speech: phonation and articulation in the human motor cortex. *Brain and Cognition*, 70(1), 31–41.

Burzynska, A. Z., Preuschhof, C., Bäckman, L., Nyberg, L., Li, S.-C., Lindenberger, U., et al. (2010). Age-related differences in white matter microstructure: region-specific patterns of diffusivity. *NeuroImage*, 49(3), 2104–2112.

Cai, S., Tourville, J. A., Beal, D. S., Perkell, J. S., Guenther, F. H., & Ghosh, S. S. (2014). Diffusion imaging of cerebral white matter in persons who stutter: evidence for network-level anomalies. *Frontiers in Human Neuroscience*, 8, 54.

Catani, M., Allin, M. P., Husain, M., Pugliese, L., Mesulam, M. M., Murray, R. M., et al. (2007). Symmetries in human brain language pathways correlate with verbal recall. *Proceedings of the National Academy of Sciences of the United States of America*, 104(43), 17163–17168.

Catani, M., Dell'Acqua, F., Vergani, F., Malik, F., Hodge, H., & Roy, P. (2012). Short frontal lobe connections of the human brain. *Cortex*, 48(2), 273–291.

Catani, M., Jones, D. K., & Ffytche, D. H. (2005). Perisylvian language networks of the human brain. *Annals of Neurology*, 57(1), 8–16.

Catani, M., & Mesulam, M. (2008). The arcuate fasciculus and the disconnection theme in language and aphasia: history and current state. *Cortex*, 44(8), 953–961.

- Catani, M., Mesulam, M. M., Jakobsen, E., Malik, F., Martersteck, A., Wieneke, C., et al. (2013). A novel frontal pathway underlies verbal fluency in primary progressive aphasia. *Brain*, 136(8), 2619–2628.
- Chang, S. E., Erickson, K. I., Ambrose, N. G., Hasegawa-Johnson, M. A., & Ludlow, C. L. (2008). Brain anatomy differences in childhood stuttering. *NeuroImage*, 39(3), 1333–1344.
- Chang, S. E., Horwitz, B., Ostuni, J., Reynolds, R., & Ludlow, C. L. (2011). Evidence of left inferior frontal premotor structural and functional connectivity deficits in adults who stutter. *Cerebral Cortex*, 21(11), 2507–2518.
- Chang, S. E., Kenney, M. K., Loucks, T. M. J., & Ludlow, C. L. (2009). Brain activation abnormalities during speech and non-speech in stuttering speakers. *NeuroImage*, 46(1), 201–212.
- Chang, S. E., Synnestvedt, A., Ostuni, J., & Ludlow, C. L. (2010). Similarities in speech and white matter characteristics in idiopathic developmental stuttering and adult-onset stuttering. *Journal of Neurolinguistics*, 23(5), 455–469.
- Choo, A. L., Chang, S. E., Zengin-Bolat kale, H., Ambrose, N. G., & Loucks, T. M. (2012). Corpus callosum morphology in children who stutter. *Journal of Communication Disorders*, 45(4), 279–289.
- Choo, A. L., Kraft, S. J., Olivero, W., Ambrose, N. G., Sharma, H., Chang, S. E., et al. (2011). Corpus callosum differences associated with persistent stuttering in adults. *Journal of Communication Disorders*, 44(4), 470–477.
- Cieslak, M., Ingham, R. J., Ingham, J. C., & Grafton, S. T. (2015). Anomalous white matter morphology in adults who stutter. *Journal of Speech, Language, and Hearing Research*, 58(2), 268–277.
- Civier, O., Bullock, D., Max, L., & Guenther, F. H. (2013). Computational modeling of stuttering caused by impairments in a basal ganglia thalamo-cortical circuit involved in syllable selection and initiation. *Brain and Language*, 126(3), 263–278.
- Civier, O., Kronfeld-Duenias, V., Amir, O., Ezrati-Vinacour, R., & Ben-Shachar, M. (2015). Reduced fractional anisotropy in the anterior corpus callosum is associated with reduced speech fluency in persistent developmental stuttering. *Brain and Language*, 143, 20–31.
- Connally, E. L., Ward, D., Howell, P., & Watkins, K. E. (2014). Disrupted white matter in language and motor tracts in developmental stuttering. *Brain and Language*, 6(3), 256–266.
- Cummine, J., Dai, W., Borowsky, R., Gould, L., Rollans, C., & Boliek, C. (2015). Investigating the ventral-lexical, dorsal-sublexical model of basic reading processes using diffusion tensor imaging. *Brain Structure and Function*, 220(1), 445–455.
- Cykowski, M. D., Fox, P. T., Ingham, R. J., Ingham, J. C., & Robin, D. A. (2010). A study of the reproducibility and etiology of diffusion anisotropy differences in developmental stuttering: a potential role for impaired myelination. *NeuroImage*, 52(4), 1495–1504.
- De Santis, S., Drakesmith, M., Bells, S., Assaf, Y., & Jones, D. K. (2014). Why diffusion tensor MRI does well only some of the time: variance and covariance of white matter tissue microstructure attributes in the living human brain. *NeuroImage*, 89, 35–44.
- Deutsch, G. K., Dougherty, R. F., Bammer, R., Siok, W. T., Gabrieli, J. D., & Wandell, B. (2005). Children's reading performance is correlated with white matter structure measured by diffusion tensor imaging. *Cortex*, 41(3), 354–363.
- Dick, A. S., Bernal, B., & Tremblay, P. (2013). The language connectome: new pathways, new concepts. *The Neuroscientist*, 20(5), 453–467.
- Dougherty, R. F., Ben-Shachar, M., Deutsch, G. K., Hernandez, A., Fox, G. R., & Wandell, B. A. (2007). Temporal-callosal pathway diffusivity predicts phonological skills in children. *Proceedings of the National Academy of Sciences of the United States of America*, 104(20), 8556–8561.
- Efron, B., & Tibshirani, R. J. (1993). *An introduction to the bootstrap*. CRC Press.
- Friederici, A. D. (2009). Pathways to language: fiber tracts in the human brain. *Trends in Cognitive Sciences*, 13(4), 175–181.
- Friston, K. J., & Ashburner, J. (2004). Generative and recognition models for neuroanatomy. *NeuroImage*, 23(1), 21–24.
- Geschwind, N. (1970). The organization of language and the brain. *Science*, 170(961), 940–944.
- Halag-Milo, T., Stoppelman, N., Kronfeld-Duenias, V., Civier, O., Amir, O., Ezrati-Vinacour, R., & Ben-Shachar, M. (2016). Beyond production: Brain responses during speech perception in adults who stutter. *NeuroImage: Clinical*, 11, 328–338.
- Hickok, G. (2012). Computational neuroanatomy of speech production. *Nature Reviews Neuroscience*, 13(2), 135–145.
- Hickok, G., & Poeppel, D. (2004). Dorsal and ventral streams: a framework for understanding aspects of the functional anatomy of language. *Cognition*, 92(1–2), 67–99.
- Hickok, G., & Poeppel, D. (2007). The cortical organization of speech processing. *Nature Reviews Neuroscience*, 8(5), 393–402.
- Hofstetter, S., Tavor, I., Tzur-Moryosef, S. T., & Assaf, Y. (2013). Short-term learning induces white matter plasticity in the fornix. *The Journal of Neuroscience*, 33(31), 12844–12850.
- Jäncke, L., Hänggi, J., & Steinmetz, H. (2004). Morphological brain differences between adult stutterers and non-stutterers. *BMC Neurology*, 4(1), 23.
- Johnson, R. T., Yeatman, J. D., Wandell, B. A., Buonocore, M. H., Amaral, D. G., & Nordahl, C. W. (2014). Diffusion properties of major white matter tracts in young, typically developing children. *NeuroImage*, 88, 143–154.
- Jones, D. K. (2004). The effect of gradient sampling schemes on measures derived from diffusion tensor MRI: a Monte Carlo study. *Magnetic Resonance in Medicine*, 51(4), 807–815.
- Jones, D. K., Knösche, T. R., & Turner, R. (2013). White matter integrity, fiber count, and other fallacies: the do's and don'ts of diffusion MRI. *NeuroImage*, 73, 239–254.
- Kell, C. A., Neumann, K., von Kriegstein, K., Posenenske, C., von Gudenberg, A. W., Euler, H., et al. (2009). How the brain repairs stuttering. *Brain*, 132, 2747–2760.
- Kemerdere, R., de Champfleure, N. M., Deverdun, J., Cochereau, J., Moritz-Gasser, S., Herbet, G., et al. (2016). Role of the left frontal aslant tract in stuttering: a brain stimulation and tractographic study. *Journal of Neurology*, 263(1), 157–167.
- Klingberg, T., Hedehus, M., Temple, E., Salz, T., Gabrieli, J., Moseley, M. E., et al. (2000). Microstructure of temporo-parietal white matter as a basis for reading ability: evidence from diffusion tensor magnetic resonance imaging. *Neuron*, 25(2), 493–500.
- Kronfeld-Duenias, V., Amir, O., Ezrati-Vinacour, R., Civier, O., & Ben-Shachar, M. (2016). The frontal aslant tract underlies speech fluency in persistent developmental stuttering. *Brain Structure and Function*, 221(1), 365–381.
- Kümmerer, D., Hartwigsen, G., Kellmeyer, P., Glauche, V., Mader, I., Klöppel, S., et al. (2013). Damage to ventral and dorsal language pathways in acute aphasia. *Brain*, 136(2), 619–629.
- Kushner, H. I. (2012). Retraining left-handers and the aetiology of stuttering: the rise and fall of an intriguing theory. *Laterality: Asymmetries of Body, Brain and Cognition*, 17(6), 673–693.
- Lebel, C., & Beaulieu, C. (2009). Lateralization of the arcuate fasciculus from childhood to adulthood and its relation to cognitive abilities in children. *Human Brain Mapping*, 30(11), 3563–3573.
- Lebel, C., Benner, T., & Beaulieu, C. (2012). Six is enough? Comparison of diffusion parameters measured using six or more diffusion-encoding gradient directions with deterministic tractography. *Magnetic Resonance in Medicine*, 68(2), 474–483.

- Leemans, A., & Jones, D. K. (2009). The B-matrix must be rotated when correcting for subject motion in DTI data. *Magnetic Resonance in Medicine*, 61(6), 1336–1349.
- Lu, C., Chen, C., Ning, N., Ding, G., Guo, T., Peng, D., et al. (2010). The neural substrates for atypical planning and execution of word production in stuttering. *Experimental Neurology*, 221(1), 146–156.
- Lu, C., Chen, C., Peng, D., You, W., Zhang, X., Ding, G., et al. (2012). Neural anomaly and reorganization in speakers who stutter: a short-term intervention study. *Neurology*, 79(7), 625–632.
- Max, L., Guenther, F., Gracco, V., Ghash, S., & Wallace, M. (2004). Unstable or insufficiently activated internal models and feedback biased motor control as sources of dysfluency: a theoretical model of stuttering. *Contemporary Issues in Communication Science and Disorders*, 31(31), 105–122.
- Mezer, A., Yeatman, J. D., Stikov, N., Kay, K. N., Cho, N. J., Dougherty, R. F., et al. (2013). Quantifying the local tissue volume and composition in individual brains with MRI. *Nature Medicine*, 19(12), 1667–1672.
- Mori, S., Crain, B. J., Chacko, V., & Van Zijl, P. (1999). Three-dimensional tracking of axonal projections in the brain by magnetic resonance imaging. *Annals of Neurology*, 45(2), 265–269.
- Namasivayam, A. K., & van Lieshout, P. (2011). Speech motor skill and stuttering. *Journal of Motor Behavior*, 43(6), 477–489.
- Nichols, T. E., & Holmes, A. P. (2002). Nonparametric permutation tests for functional neuroimaging: a primer with examples. *Human Brain Mapping*, 15(1), 1–25.
- Oldfield, R. C. (1971). The assessment and analysis of handedness: the Edinburgh inventory. *Neuropsychologia*, 9(1), 97–113.
- Poepfel, D., Emmorey, K., Hickok, G., & Pylkkänen, L. (2012). Towards a new neurobiology of language. *The Journal of Neuroscience*, 32(41), 14125–14131.
- Preibisch, C., Neumann, K., Raab, P., Euler, H., von Gudenberg, A., Lanfermann, H., et al. (2003). Evidence for compensation for stuttering by the right frontal operculum. *NeuroImage*, 20(2), 1356–1364.
- Price, C. J. (2000). The anatomy of language: contributions from functional neuroimaging. *Journal of Anatomy*, 197(3), 335–359.
- Riley, G. (1994). *Stuttering severity instrument for children and adults* (3rd ed.). Austin, Texas: Pro-Ed.
- Rohde, G. K., Barnett, A. S., Bassler, P. J., Marenco, S., & Pierpaoli, C. (2004). Comprehensive approach for correction of motion and distortion in diffusion-weighted MRI. *Magnetic Resonance in Medicine*, 51(1), 103–114.
- Sasson, E., Doniger, G., Pasternak, O., & Assaf, Y. (2010). Structural correlates of memory performance with diffusion tensor imaging. *NeuroImage*, 50(3), 1231–1242.
- Sasson, E., Doniger, G., Pasternak, O., Tarrasch, R., & Assaf, Y. (2012). Structural correlates of cognitive domains in normal aging with diffusion tensor imaging. *Brain Structure and Function*, 217(2), 503–515.
- Sasson, E., Doniger, G., Pasternak, O., Tarrasch, R., & Assaf, Y. (2013). White matter correlates of cognitive domains in normal aging with diffusion tensor imaging. *Frontiers in Neuroscience*, 7, 32.
- Saur, D., Kreher, B. W., Schnell, S., Kummerer, D., Kellmeyer, P., Vry, M. S., et al. (2008). Ventral and dorsal pathways for language. *Proceedings of the National Academy of Sciences of the United States of America*, 105(46), 18035–18040.
- Sommer, M., Koch, M. A., Paulus, W., Weiller, C., & Büchel, C. (2002). Disconnection of speech-relevant brain areas in persistent developmental stuttering. *The Lancet*, 360(9330), 380–383.
- Stikov, N., Perry, L. M., Mezer, A., Rykhlevskaia, E., Wandell, B. A., Pauly, J. M., et al. (2011). Bound pool fractions complement diffusion measures to describe white matter micro and macrostructure. *NeuroImage*, 54(2), 1112–1121.
- Tavor, I., Yablonski, M., Mezer, A., Rom, S., Assaf, Y., & Yovel, G. (2014). Separate parts of occipito-temporal white matter fibers are associated with recognition of faces and places. *NeuroImage*, 86, 123–130.
- Travis, L. E. (1931). *Speech pathology*. New York: Appleton-Century.
- Travis, K. E., Leitner, Y., Feldman, H., & Ben-Shachar, M. (2014). Cerebellar white matter pathways are associated with reading skills in children and adolescents. *Human Brain Mapping*, 36(4), 1536–1553.
- Wahl, M., Li, Y. O., Ng, J., Lahue, S. C., Cooper, S. R., Sherr, E. H., et al. (2010). Microstructural correlations of white matter tracts in the human brain. *NeuroImage*, 51(2), 531–541.
- Wakana, S., Caprihan, C., Panzenboeck, M. M., Fallon, J. H., Perry, M., Gollub, R. L., et al. (2007). Reproducibility of quantitative tractography methods applied to cerebral white matter. *NeuroImage*, 36(3), 630–644.
- Watkins, K. E., Smith, S. M., Davis, S., & Howell, P. (2008). Structural and functional abnormalities of the motor system in developmental stuttering. *Brain*, 131(1), 50–59.
- Xuan, Y., Meng, C., Yang, Y., Zhu, C., Wang, L., Yan, Q., et al. (2012). Resting-state brain activity in adult males who stutter. *PLoS One*, 7(1), e30570.
- Yeatman, J. D., Dougherty, R. F., Ben-Shachar, M., & Wandell, B. A. (2012). Development of white matter and reading skills. *Proceedings of the National Academy of Sciences of the United States of America*, 109(44), E3045–E3053.
- Yeatman, J. D., Dougherty, R. F., Myall, N. J., Wandell, B. A., & Feldman, H. M. (2012). Tract profiles of white matter properties: automating fiber-tract quantification. *PLoS One*, 7(11), e49790.
- Yeatman, J. D., Dougherty, R. F., Rykhlevskaia, E., Sherbondy, A. J., Deutsch, G. K., Wandell, B. A., et al. (2011). Anatomical properties of the arcuate fasciculus predict phonological and reading skills in children. *Journal of Cognitive Neuroscience*, 23(11), 3304–3317.